Tuning the thermal conductivity of graphene nanoribbons by edge passivation and isotope engineering: A molecular dynamics study

Jiuning Hu,[1,a)] Stephen Schiffli,[2] Ajit Vallabhaneni,[3] Xiulin Ruan,[4] and Yong P. Chen[5,b)]

[1]*School of Electrical and Computer Engineering, Birck Nanotechnology Center, Purdue University, West Lafayette, Indiana 47907, USA*
[2]*School of Electrical and Computer Engineering, Purdue University, West Lafayette, Indiana 47907, USA*
[3]*School of Mechanical Engineering, Purdue University, West Lafayette, Indiana 47907, USA*
[4]*School of Mechanical Engineering, Birck Nanotechnology Center, Purdue University, West Lafayette, Indiana 47907, USA*
[5]*Department of Physics, Birck Nanotechnology Center, School of Electrical and Computer Engineering, Purdue University, West Lafayette, Indiana 47907, USA*

Using classical molecular dynamics simulation, we have studied the effect of edge-passivation by hydrogen (H-passivation) and isotope mixture (with random or superlattice distributions) on the thermal conductivity of rectangular graphene nanoribbons (GNRs) (of several nanometers in size). We find that the thermal conductivity is considerably reduced by the edge H-passivation. We also find that the isotope mixing can reduce the thermal conductivities, with the superlattice distribution giving rise to more reduction than the random distribution. These results can be useful in nanoscale engineering of thermal transport and heat management using GNRs. © *2010 American Institute of Physics*. [doi:10.1063/1.3491267]

Graphene[1,2] is a monolayer of graphite with a honeycomb lattice structure. It exhibits many unique properties and has drawn intense attention in the past few years. The unusual electronic properties of graphene are promising in many fundamental studies and applications, e.g., the ultrahigh electron mobility[2] and the tunable band gap and magnetic properties by the size and edge chirality of graphene nanoribbons (GNRs).[3–6] Graphene also has remarkable thermal properties. The measured value of thermal conductivity of graphene reaches as high as several thousand of watt per meter Kelvin,[7–10] among the highest values of known materials. Previous studies[11–13] show that the thermal transport in GNRs depends on the edge chirality of GNRs. In realistic graphene samples, the edges are often passivated[14–16] and the isotope composition can be controlled.[17] Motivated by these, we study the effect of the edge H-passivation and various isotope distributions on the thermal transport in GNRs. We find that the thermal conductivity can be reduced by the edge H-passivation and tuned by the isotope distributions. Our study is useful in nanoscale control and management of thermal transport by engineering the chemical composition of GNRs.

In this work, we employ the classical molecular dynamics (MD, similar to the method in Ref. 11) to calculate the thermal conductivities of GNRs. We use the Brenner potential,[18] which incorporates the many-body carbon-carbon and carbon-hydrogen interactions by introducing a fractional number of covalent bonds. This method has been applied to many carbon-based systems,[19,20] especially to graphene.[11,21,22] The structures of GNRs are shown in Fig. 1 (with edge H-passivation) and the insets of Fig. 3 (with isotope mixtures). We use fixed boundary conditions, i.e., the atoms denoted by squares are fixed at their equilibrium positions. The atoms denoted by left- and right-pointing tri-

angles are placed in two Nosé–Hoover[23,24] thermostats at different temperatures. The thermal conductivity can be calculated from the Fourier law $\kappa = Jd/(\Delta Twh)$, where ΔT is the temperature difference (chosen to be in the linear response regime[25]) between two thermostats, J is the resulting thermal current, d is the length, w is the width, and $h(=0.335$ nm$)$ is the thickness of GNRs, respectively. Calculations presented below are performed for representative GNRs with $d \sim 6$ nm and $w \sim 1.5$ nm. All the calculated thermal conductivities are normalized by $\kappa_0(\sim 670$ W/m K$)$ which is the thermal conductivity calculated at 100 K for the pure ^{12}C GNR with armchair edge and without H-passivation [shown in Fig. 1(a) in Ref. 26]. Although the specific value of κ_0 depends on the GNR size,[25] the choice of thermostat and boundary condition in MD simulation,[12,27] we have checked that our conclusions and the qualitative behavior of κ discussed below do not. The equations of motion for atoms
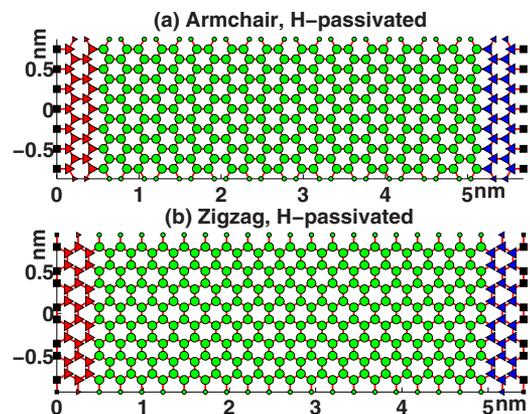

FIG. 1. (Color online) Structure of hydrogen-passivated armchair (a) and zigzag (b) GNRs. The hydrogen atoms are denoted by smaller symbols while the ^{12}C atoms are denoted by larger ones. ■ denotes fixed boundary atoms. ▶ (◀) denotes atoms in the left (right) thermostat. ● denotes the remaining atoms in the bulk.

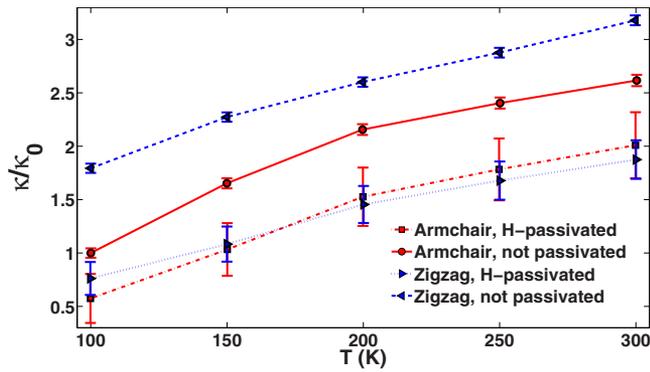a)Electronic mail: hu49@purdue.edu.
b)Electronic mail: yongchen@purdue.edu.

FIG. 2. (Color online) Temperature dependent thermal conductivity of GNRs with and without edge H-passivation.

FIG. 3. (Color online) Temperature dependent thermal conductivity of GNRs with ^{13}C isotopes distributed (a) randomly and (b) in a superlattice structure. The insets show the corresponding typical structures of GNRs with the same meaning of symbols as that in Fig. 1. The larger (smaller) symbols denote ^{13}C (^{12}C) atoms.

labeled by triangles in either left or right Nosé–Hoover thermostat are the following:

$$\frac{d}{dt}\mathbf{p}_i = \mathbf{F}_i - \gamma\mathbf{p}_i, \quad \frac{d}{dt}\gamma = \frac{T(t) - T_0}{\tau^2 T_0}, \tag{1}$$

where i runs over all the atoms in the thermostat, $\mathbf{p}_i$ is the momentum of the i-th atom, $\mathbf{F}_i$ is the total force acting on the i-th atom, γ is the dynamic parameter of the thermostat with initial value of zero, τ is the relaxation time of the thermostat, $T(t) \equiv 2/3Nk_B\Sigma_i \frac{\mathbf{p}_i^2}{2m_i}$ is the actual temperature of atoms in the thermostat at time instant t, $T_0 = T_L$ (or T_R) is the desired temperature of the left (or right) thermostat, N is the number of atoms in the thermostat, k_B is the Boltzmann constant and m_i is the mass of the i-th atom. The atoms labeled by circles obey the Newton's law of motion with $\gamma = 0$. The carbon-carbon potential is the same for all carbon isotopes.

We study the temperature dependent thermal conductivity of H-passivated GNRs. All of our simulation results indicate that the thermal conductivity increases with temperature. This behavior is consistent with our previous work[11] and the recent prediction about the size-dependent behavior of thermal conductivities in graphene flakes.[28] Figure 1 shows the armchair and zigzag GNRs with top and bottom edges H-passivated. As shown in Fig. 2, the edge H-passivation significantly reduces the thermal conductivity, compared to the nonpassivated GNRs. A recent study[29] using equilibrium MD has obtained similar conclusions. We note that the error bars (related to MD fluctuations) for H-passivated GNRs are considerably larger than that for the nonpassivated GNRs, probably due to the much smaller mass of hydrogen atoms.

We also study the effect of the mixture of carbon isotopes ^{12}C and ^{13}C on the thermal conductivity of GNRs. Here, we demonstrate the results in the case of armchair GNRs (qualitatively similar results are obtained for zigzag GNRs). The concentration of ^{13}C is $N_{13}/(N_{12}+N_{13})$, where $N_{12/13}$ is the number of $^{12/13}$C atoms. The thermal conductivity is seen to be reduced by introducing ^{13}C, and the thermal conductivity of pure ^{13}C GNRs is lower than that of pure ^{12}C GNRs because ^{13}C atoms have larger mass and thus give lower phonon frequency.[30] The inset of Fig. 3(a) shows a typical random isotope distribution. Another isotope distribution pattern we study is the isotopic superlattice structure shown in the inset of Fig. 3(b). Here, the whole GNR is composed of four slices with equal length and the same isotope composition. Within each slice [such as the dashed box
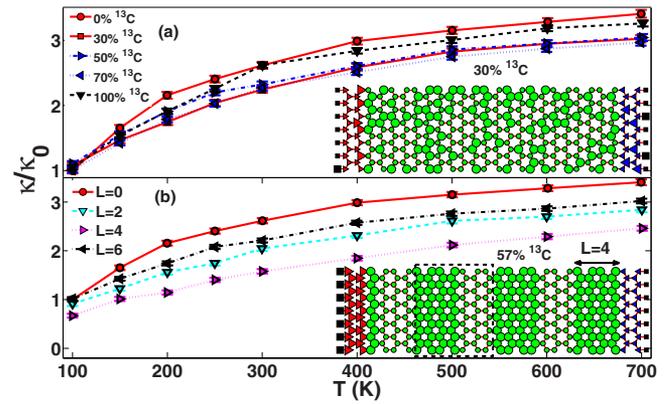
in the inset of Fig. 3(b)], the number (L) of vertical ^{13}C atomic chains with zigzag shape [e.g., $L=4$ for the inset of Fig. 3(b)] can vary from 0 to 7 (see details in Ref. 26). $L=0(L=7)$ corresponds to the pure ^{12}C (^{13}C) GNR. The temperature dependent thermal conductivity in Fig. 3 shows that the isotope effect becomes more evident at higher temperatures. We show the thermal conductivity as a function of the concentration of ^{13}C calculated at the temperature of 500 K in Fig. 4. In the case of the random distributions, the calculated thermal conductivity is an average of 10 different distributions with the same isotope concentration. For random isotope distributions, the isotope concentration dependent thermal conductivity (dashed line in Fig. 4) shows a pan shape and is relatively flat in the concentration range of $\sim 20\%-90\%$. The thermal conductivity is reduced by $\sim 10\%$ around the isotope concentration of $\sim 50\%$. The error bars are determined from the deviations of the thermal conductivities for the ten different distributions from their average value. In contrast, the conical shape of the solid line in Fig. 4 shows much stronger dependence of the thermal conductivity on the isotope concentration for the superlattice structures, with $\sim 30\%$ reduction in the thermal conductivity at $\sim 50\%$ of the isotope concentration. We have also obtained similar results using velocity exchange MD (Ref. 31) in the LAMMPS package.[32]

It has been previously demonstrated that the thermal conductivity depends on the edge chirality[11–13] in the ab-
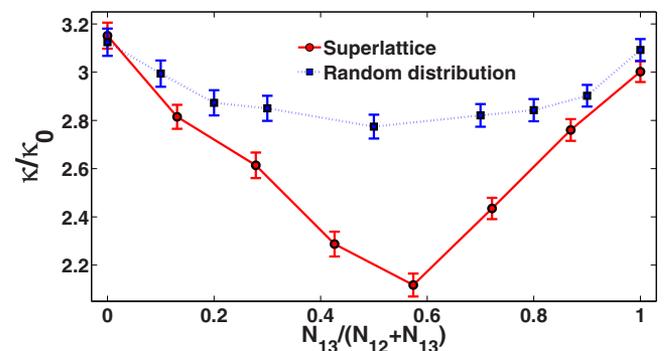

FIG. 4. (Color online) Thermal conductivity as a function of the ^{13}C concentration for superlattice (solid line) and random (dashed line) isotope distributions.

sence of H-passivation, i.e., the thermal conductivity of the zigzag GNR is larger than that of the armchair GNR. However, as shown in Fig. 2, their thermal conductivities become close to each other within the MD error bars after the H-passivation, suggesting that phonon scattering with the hydrogenated edges dominates over the contribution from the chirality effect. We have suggested that the smaller thermal conductivity of armchair GNRs is due to the stronger phonon scattering at the armchair edges.[11] It is interesting to note that the H-passivated zigzag GNR in Fig. 1(b) resembles the armchair GNRs at the edges. We suggest that the thermal transport in small GNRs (several nanometers in size in our study) is strongly affected by the edge configuration.

Recently, it has been experimentally demonstrated that different carbon isotopes can be controllably introduced in graphene, such as ^{13}C, in the chemical vapor deposition growth of graphene on metals. Both random and segregation (by domains of different isotopes) distributions have been observed.[17] This opens possibilities of engineering the thermal properties of graphene by isotope distributions. The isotope effect on the thermal transport has been studied in several nanomaterials, such as carbon nanotubes,[33,34] boron nitride nanotubes,[35,36] and silicon nanowires.[37] The pan shape of the dashed line in Fig. 4 is consistent with the reduction of the thermal conductivity in the "alloy limit."[38] A similar pan shape is found in GNRs (Ref. 39) and SiGe nanowires[40] by tuning the composition. By keeping the isotope concentration a constant of ~50%, it has been shown[41] that the thermal conductivity as a function of the slice length (which is kept constant in our simulations) gives similar conical shaped dependence as we see in Fig. 4 for the superlattice structures.

In conclusion, the classical MD is applied to calculate the thermal conductivities of rectangular GNRs. We find that the edge H-passivation can reduce the thermal conductivity significantly. We also show that the thermal conductivity depends on the concentrations of isotopic atoms and their distribution patterns. The isotopic superlattice distributions can reduce the thermal conductivity much more than random distributions. These findings can be useful in controlling heat transfer in nanoscale using GNR-based thermal devices.

[1]A. K. Geim and K. S. Novoselov, Nature Mater. **6**, 183 (2007).
[2]A. H. C. Neto, F. Guinea, N. M. R. Peres, K. S. Novoselov, and A. K. Geim, Rev. Mod. Phys. **81**, 109 (2009).
[3]K. Nakada, M. Fujita, G. Dresselhaus, and M. S. Dresselhaus, Phys. Rev. B **54**, 17954 (1996).
[4]Y. W. Son, M. L. Cohen, and S. G. Louie, Nature (London) **444**, 347 (2006).
[5]M. Y. Han, B. Ozyilmaz, Y. Zhang, and P. Kim, Phys. Rev. Lett. **98**, 206805 (2007).
[6]Z. Chen, Y. M. Lin, M. J. Rooks, and P. Avouris, Physica E **40**, 228 (2007).
[7]A. A. Balandin, S. Ghosh, W. Bao, I. Calizo, D. Teweldebrhan, F. Miao, and C. N. Lau, Nano Lett. **8**, 902 (2008).
[8]W. Cai, A. L. Moore, Y. Zhu, X. Li, S. Chen, L. Shi, and R. S. Ruoff, Nano Lett. **10**, 1645 (2010).
[9]C. Faugeras, B. Faugeras, M. Orlita, M. Potemski, R. R. Nair, and A. K. Geim, ACS Nano **4**, 1889 (2010).
[10]L. A. Jauregui, Y. Yue, A. N. Sidorov, J. Hu, Q. Yu, G. Lopez, R. Jalilian, D. K. Benjamin, D. A. Delk, W. Wu, Z. Liu, X. Wang, Z. Jiang, X. Ruan, J. Bao, S. S. Pei, and Y. P. Chen, ECS Trans. **28**(5), 73 (2010).
[11]J. Hu, X. Ruan, and Y. P. Chen, Nano Lett. **9**, 2730 (2009).
[12]J.-W. Jiang, J. Chen, J.-S. Wang, and B. Li, Phys. Rev. B **80**, 052301 (2009).
[13]Y. Xu, X. Chen, B.-L. Gu, and W. Duan, Appl. Phys. Lett. **95**, 233116 (2009).
[14]S. Park and R. S. Ruoff, Nat. Nanotechnol. **4**, 217 (2009).
[15]D. W. Boukhvalov and M. I. Katsnelson, J. Phys.: Condens. Matter **21**, 344205 (2009).
[16]Y. H. Lu, R. Q. Wu, L. Shen, M. Yang, Z. D. Sha, Y. Q. Cai, P. M. He, and Y. P. Feng, Appl. Phys. Lett. **94**, 122111 (2009).
[17]X. Li, W. Cai, L. Colombo, and R. S. Ruoff, Nano Lett. **9**, 4268 (2009).
[18]D. W. Brenner, Phys. Rev. B **42**, 9458 (1990).
[19]X. Gong, J. Li, H. Zhang, R. Wan, H. Lu, S. Wang, and H. Fang, Phys. Rev. Lett. **101**, 257801 (2008).
[20]X. H. Zhang, G. E. Santoro, U. Tartaglino, and E. Tosatti, Phys. Rev. Lett. **102**, 125502 (2009).
[21]C. Y. Wang, K. Mylvaganam, and L. C. Zhang, Phys. Rev. B **80**, 155445 (2009).
[22]Z.-Y. Ong and E. Pop, Phys. Rev. B **81**, 155408 (2010).
[23]S. Nosé, J. Chem. Phys. **81**, 511 (1984).
[24]W. G. Hoover, Phys. Rev. A **31**, 1695 (1985).
[25]J. Hu, X. Ruan, Z. Jiang, and Y. P. Chen, *Frontiers of Characterization and Metrology for Nanoelectronics 2009*, AIP Conf. Proc. No. 1173 (AIP, New York, 2009), p. 135.
[26]See supplementary material at http://dx.doi.org/10.1063/1.3491267 for the isotope superlattice structures.
[27]J. Chen, G. Zhang, and B. Li, J. Phys. Soc. Jpn. **79**, 074604 (2010).
[28]D. L. Nika, S. Ghosh, E. P. Pokatilov, and A. A. Balandin, Appl. Phys. Lett. **94**, 203103 (2009).
[29]W. J. Evans, L. Hu, and P. Keblinski, Appl. Phys. Lett. **96**, 203112 (2010).
[30]N. W. Ashcroft and N. D. Mermin, *Solid State Physics* (Holt, Rinehart, and Winston, New York, 1976).
[31]F. Müller-Plathe, J. Chem. Phys. **106**, 6082 (1997).
[32]S. J. Plimpton, J. Comput. Phys. **117**, 1 (1995).
[33]G. Zhang and B. Li, J. Chem. Phys. **123**, 114714 (2005).
[34]G. Stoltz, N. Mingo, and F. Mauri, Phys. Rev. B **80**, 113408 (2009).
[35]C. W. Chang, A. M. Fennimore, A. Afanasiev, D. Okawa, T. Ikuno, H. Garcia, D. Li, A. Majumdar, and A. Zettl, Phys. Rev. Lett. **97**, 085901 (2006).
[36]D. A. Stewart, I. Savic, and N. Mingo, Nano Lett. **9**, 81 (2009).
[37]N. Yang, G. Zhang, and B. Li, Nano Lett. **8**, 276 (2008).
[38]W. Kim, J. Zide, A. Gossard, D. Klenov, S. Stemmer, A. Shakouri, and A. Majumdar, Phys. Rev. Lett. **96**, 045901 (2006).
[39]J.-W. Jiang, J. Lan, J.-S. Wang, and B. Li, J. Appl. Phys. **107**, 054314 (2010).
[40]J. Chen, G. Zhang, and B. Li, Appl. Phys. Lett. **95**, 073117 (2009).
[41]T. Ouyang, Y. P. Chen, K. K. Yang, and J. X. Zhong, Europhys. Lett. **88**, 28002 (2009).